

Submitted to the Astrophysical Journal Letters

## TEMPORAL VARIATION IN THE ABUNDANCE OF EXCITED $\text{Fe}^+$ NEAR A GRB AFTERGLOW

Miroslava Dessauges-Zavadsky<sup>1</sup>, Hsiao-Wen Chen<sup>2</sup>, Jason X. Prochaska<sup>3</sup>, Joshua S. Bloom<sup>4</sup>,  
Aaron J. Barth<sup>5</sup>

### ABSTRACT

Excited  $\text{Si}^+$  and  $\text{Fe}^+$  species are routinely observed in the host environment of  $\gamma$ -ray burst (GRB) afterglows, but are not commonly seen in other extragalactic locations. Their presence signals unusual properties in the gaseous environment of these GRB hosts that arise either as a result of the intense ionizing radiation of the afterglow or through collision excitation in a dense cloud. In particular, the photon pumping scenario has explicit expectations for temporal variation in the strength of the excited lines, owing to the decline in the ionizing flux of the GRB afterglow. We analyze afterglow spectra of GRB 020813 obtained in two epochs of  $\approx 16$  hours apart, and examine transitions from the first excited state of  $\text{Fe}^+$  at  $J = 7/2$  in these two sets of data. We report a significant decline by at least a factor of five in the equivalent width of the  $\text{Fe II } \lambda 2396$  transition, the strongest from the  $J = 7/2$  state. We perform a Monte-Carlo analysis and determine that this temporal variation is present at more than  $3\sigma$  level of significance. This observation represents the first detection in the temporal variation of the excited  $\text{Fe}^+$  states in the GRB host ISM, a direct influence of the burst itself on its environment. We further estimate that the  $\text{Fe}^+$  gas resides in 50-100 pc from the afterglow, based on the afterglow lightcurve and the presence and absence of the excited  $\text{Fe II } \lambda 2396$  in the two-epoch observations.

<sup>1</sup>Observatoire de Genève, 51 Ch. des Maillettes, 1290 Sauverny, Switzerland; miroslava.dessauges@obs.unige.ch

<sup>2</sup>Department of Astronomy & Astrophysics; University of Chicago; 5640 S. Ellis Ave., Chicago, IL 60637; hchen@oddjob.uchicago.edu

<sup>3</sup>UCO/Lick Observatory; University of California, Santa Cruz; Santa Cruz, CA 95064; xavier@ucolick.org

<sup>4</sup>Department of Astronomy, 601 Campbell Hall, University of California, Berkeley, CA 94720-3411; jbloom@astron.berkeley.edu

<sup>5</sup>Department of Physics and Astronomy, University of California at Irvine, 4129 Frederick Reines Hall, Irvine, CA 92697-4575; barth@uci.edu

*Subject headings:* gamma rays: observations — galaxies: individual (GRB 020813)  
— galaxies: ISM — line: formation

## 1. Introduction

Long-duration  $\gamma$ -Ray Bursts (GRBs) are believed to trace the death of massive, short lived stars (see Woosley & Bloom 2006, for review). The brightness of GRB afterglows for a brief period makes them visible throughout most of the observable Universe (e.g. Kawai et al. 2006) and therefore a sensitive probe of both the interstellar medium (ISM) of their host galaxies and the intervening gas (e.g Vreeswijk et al. 2004; Chen et al. 2005; Prochter et al. 2006). The study of metal absorption lines detected in the afterglow spectra illuminates the physical conditions in the ISM hosting the GRB, such as the H<sub>1</sub> column density, the gas metallicity, the dust-to-gas ratio, and the kinematics. Moreover, the access to features belonging to the circumstellar medium of the progenitor star of the GRB may yield strong constraints on the progenitor and may help to understand the impact of the GRB on the local environment (e.g. Ramirez-Ruiz et al. 2005; van Marle, Langer, & Graciá-Segura 2005; Prochaska, Chen, & Bloom 2006, hereafter PCB06).

Interestingly, the transitions from excited states of C<sup>+</sup>, Si<sup>+</sup>, and O<sup>0</sup> appear to be a generic feature in GRB host environments, while they are observed through only rare sightlines, such as broad absorption-line (BAL) quasars (Hall et al. 2002), and in gas near stars like  $\eta$  Carinae and  $\beta$  Pictoris (Gull et al. 2005; Lagrange-Henri, Vidal-Madjar & Ferlet 1988). In addition, a large fraction of the GRB hosts also show excited Fe<sup>+</sup> lines (Prochaska et al. 2006). Does the detection of these excited state absorption lines reveal extreme (pre) circumburst environments or are they the result of work done by the afterglow in early times after the burst? To answer this we need to consider competing scenarios for the production of excited-state transitions, and particularly for Fe<sup>+</sup>: (1) collisional excitation and (2) photon pumping. PCB06 have recently shown that in the presence of an intensified UV radiation field from the afterglow – known to be stronger than 10<sup>5</sup> to 10<sup>6</sup> times the ambient far-UV radiation field in the ISM of the Milky Way – indirect UV pumping alone can produce the excited states observed in GRB hosts without imposing extreme gas density and temperature<sup>6</sup>. Under the photon pumping conditions, temporal variation in the absorption-line strength of excited state transitions is expected, because of the decline in the ionizing flux of the afterglow. Perna & Loeb (1998) and Böttcher et al. (1999) predicted time-dependent resonance

---

<sup>6</sup>A third scenario is for the bright progenitor star, such as a WR star, to UV pumping these excited Fe<sup>+</sup>. However, as we will show below, at the distance allowed for Fe<sup>+</sup> to survive the intense afterglow UV radiation ( $\sim 50$  pc) the excitation rate from the WR star is insufficient to produce the observed excited states. In addition, the excitation rate due to direct IR pumping by the afterglow is orders of magnitude smaller than the excitation rate due to afterglow UV pumping.

absorption features in the GRB afterglow spectra, such as the Mg II doublet, over a timescale of a few days to a few weeks. Their analysis also indicated that important constraints on the extent and gas density of the circumburst medium can be derived. However, searches for absorption-line variability have so far yielded null results (Vreeswijk et al. 2001; Mirabal et al. 2002).

Under the photon pumping scenario, temporal variation in excited transitions on scales of a few hours is expected, because the decay timescale for the excited states ranges from 8 to 15 minutes. Given the new insights into the origin of excited lines, in this *Letter* we analyze afterglow spectra of GRB 020813 obtained in two different epochs of  $\approx$  16 hours apart. These data sets have a suitable time coverage to serve the purpose to search for variation in the excited Fe<sup>+</sup> lines. We report a significant decline in the equivalent width of the strongest transition from the excited state Fe<sup>+</sup>  $J = 7/2$ . This observation represents the first detection in temporal variation of the excited Fe II states in GRB host ISM, lending strong support for the indirect UV pumping scenario as the primary excitation mechanism of this gas.

## 2. Observations and Data Reduction

GRB 020813 was detected by the High Energy Transient Explorer 2 (HETE 2) at 2:44 UT on 2002 August 13 (Villasenor et al. 2002; Fox, Blake & Price 2002). Two sets of spectroscopic observations were obtained for the optical afterglow: spectropolarimetry with the Low Resolution Imaging Spectrograph (LRIS; Oke et al. 1995; Goodrich 1995) on the Keck I telescope and echelle spectroscopy with the Ultraviolet-Visual Echelle Spectrograph (UVES; D’Odorico et al. 2000) on the VLT Kueyen ESO telescope. The epoch 1 LRIS data were acquired on 2002 August 13, starting at 7:23 UT (Barth et al. 2003) and spanning 3 hours in duration. The brightness of the GRB at 4.7 hours after the burst was  $R \approx 18.4$ . The observed spectral range is  $\lambda = 3200 - 9400 \text{ \AA}$  with a wavelength scale of  $1.09 \text{ \AA pixel}^{-1}$  in the blue half and  $1.86 \text{ \AA pixel}^{-1}$  in the red half. The signal-to-noise ratio per pixel achieved by combining the twelve 15 minute exposures is very good,  $S/N = 50 - 100$ .

The epoch 2 UVES data were acquired on 2002 August 13, starting at 23:32 UT 16.1 hours after the start of the LRIS observations and spanning roughly 2.1 hours in duration (Fiore et al. 2005). The brightness of the GRB was then  $R \approx 20.4$ . Two exposure times of 2300 and 3600 s were obtained with the dichroic #1 B346+R580 and one exposure of 1800 s with the dichroic #2 B437+R860. We reduced these spectra, available in the ESO Science Archive (program ID 69.A-0516), using the ESO data reduction package MIDAS and the UVES pipeline in an interactive mode. A detailed description of the pipeline can be found in Ballester et al. (2000). To optimize the results, we made a systematic check of each step of the pipeline reduction. Individual exposure spectra were weighted by their  $S/N$  ratios and co-added to form a final stacked spectrum. The

resulting UVES high-resolution spectrum extends from 4800 to 6800 Å and has a wavelength scale of  $0.029 \text{ \AA pixel}^{-1}$  in the blue half and  $0.035 \text{ \AA pixel}^{-1}$  in the red half. The achieved signal-to-noise ratio per pixel is low,  $S/N = 4 - 5$  (the  $S/N$  is even poorer at  $4800 > \lambda > 6800 \text{ \AA}$ ).

### 3. Temporal Variation

Barth et al. (2003) identified two absorption systems on the GRB 020813 line of sight at  $z = 1.255$  and  $z = 1.224$  with the former being associated with the host galaxy of the GRB. Savaglio & Fall (2004) performed a detailed abundance analysis of the GRB 020813 host ISM. They obtained the column density measurements of numerous ions detected in the LRIS spectrum – C I, Mg II, Mg I, Al II, Si II, Ti II, Cr II, Mn II, Fe II, Ni II, Zn II, and Ca II. The high-resolution UVES spectrum was analyzed by Fiore et al. (2005), where only the Mg II, Mg I, and Fe II ions are accessible.

An emerging feature of GRB environments is the presence of excited state transitions (Vreeswijk et al. 2004; Chen et al. 2005; Berger et al. 2006; Prochaska et al. 2006). For the host of GRB 020813, only the detection of the excited Si II  $\lambda 1533$  ( $J = 3/2$ ) transition was reported so far (Savaglio & Fall 2004). We show, in addition, that the excited Fe II  $\lambda 2396$  ( $J = 7/2$ ) transition, the strongest of all from the  $J = 7/2$  state (i.e., with the highest  $\lambda f$  product), is detected. We report in Table 1 measurements and upper limits for the rest-frame equivalent widths of various transitions from the  $J = 7/2$  state that are covered by both LRIS and UVES spectra. We note that the Fe II  $\lambda 2396$  line is clearly detected in the LRIS spectrum with a rest-frame equivalent width of  $0.32 \pm 0.06 \text{ \AA}$ , while the other three excited Fe<sup>+</sup> lines are only marginally detected (we provide  $2\sigma$  upper limits).

We searched for these Fe<sup>+</sup> excited state transitions in the epoch 2 UVES spectrum (the Si II  $\lambda 1533$  ( $J = 3/2$ ) line is not covered by the UVES spectrum). In contrast, the Fe II  $\lambda 2396$  line, which is well detected in the epoch 1 LRIS spectrum, is not present in the epoch 2 UVES spectrum. This is illustrated in Figs. 1 a) with the full resolution UVES spectrum and b) with the UVES spectrum smoothed and rebinned to the spectral resolution of the LRIS spectrum. We note that the LRIS spectroscopic observations were carried out using a D560 dichroic. The spectral break between the blue and red arms is located at roughly 5600 Å, much beyond the wavelengths where the excited Fe II  $\lambda 2396$  features are identified. We have also examined the 12 individual exposures from the LRIS observations. The Fe<sup>+</sup> absorption feature is detected in all exposures, and have varied only very marginally over the three hours of the spectroscopic observations.

We measured an upper limit to the rest-frame equivalent width of Fe II  $\lambda 2396$  in the UVES spectrum over the line profile observed in the LRIS spectrum. A comparison between the equivalent widths derived from the two-epoch spectra shows that the Fe<sup>+</sup> rest-frame equivalent width in

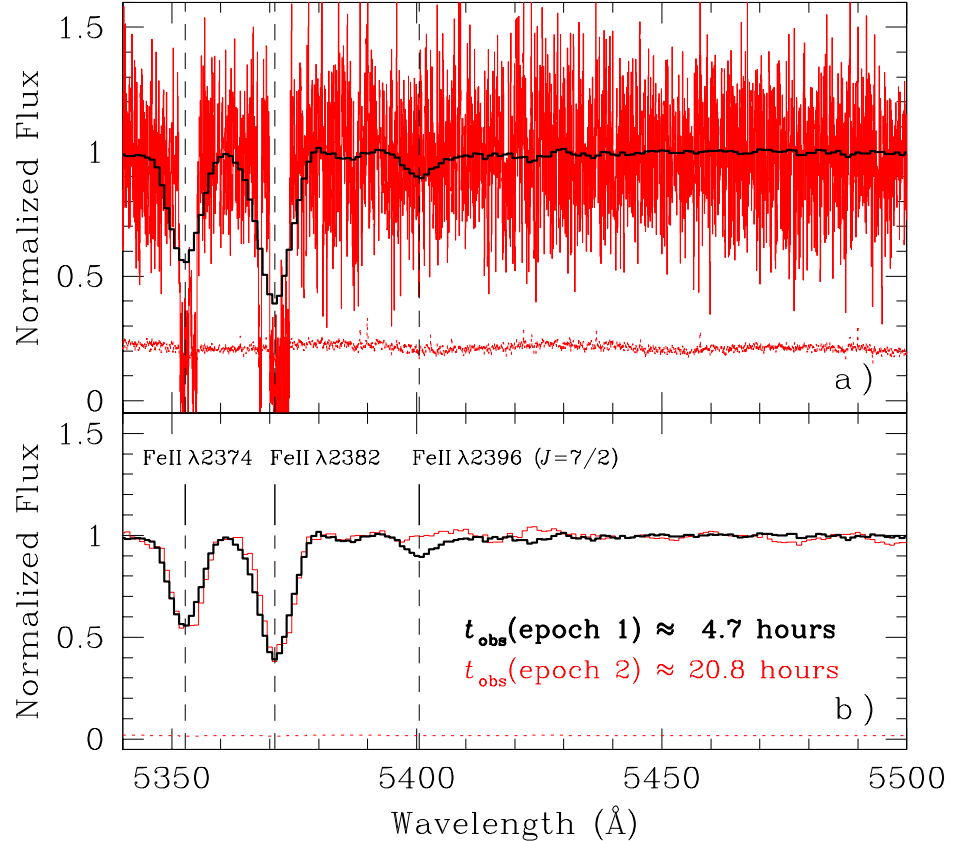


Fig. 1.— Panel a) Full resolution UVES spectrum of the GRB 020813 afterglow with its  $1\sigma$  error spectrum (thin curve) acquired  $\approx 20.8$  hours after the burst and overplotted on the low-resolution LRIS spectrum (thick curve) obtained only  $\approx 4.7$  hours after the burst. Panel b) Rebinned and smoothed UVES spectrum (thin curve) to the spectral resolution of the LRIS spectrum (thick curve) with its corresponding  $1\sigma$  error spectrum (warning: the vertical scale is different from the one used in panel a)). The dashed lines correspond to the central positions of  $\text{Fe II } \lambda 2374$ ,  $\text{Fe II } \lambda 2382$ , and the excited line  $\text{Fe II } \lambda 2396$ , respectively.  $\text{Fe II } \lambda 2396$  is clearly detected in the epoch 1 LRIS spectrum, but is not observed in the epoch 2 UVES spectrum (see Table 1 for the rest-frame equivalent width measurements).

epoch 1 of  $0.32 \text{ \AA}$  differs from the rest-frame equivalent width in epoch 2 at the  $4\sigma$  significance level. In other words, at  $> 99.999\%$  confidence level, the strength of the  $\text{Fe II } \lambda 2396$  line varied between the LRIS and UVES observations. Including a conservative estimate of the systematic error associated with continuum placement, the result remains at  $\sim 3\sigma$  significance level (see Table 1).

It is, however, necessary to test the robustness of the observed temporal variation in the excited  $\text{Fe II } \lambda 2396$  line, because of the poor signal-to-noise ratio of the UVES data and because of the different spectral resolutions between the two data sets. We therefore performed a Monte-Carlo analysis. We first adopted the LRIS spectrum as the fiducial model spectrum of the afterglow (given its very high signal-to-noise ratio) and assumed that the random noise of the UVES data is the dominant source of errors. Next, we generated a thousand synthetic spectra through random sampling the LRIS data within the UVES uncertainties. Specifically, for each pixel  $i$ , the synthetic flux was obtained by drawing a random value within the Gaussian error distribution function centered at the fiducial LRIS flux. The width of the Gaussian distribution function was set by the corresponding  $1\sigma$  error of the pixel  $i$  in the UVES spectrum.

We applied the Monte-Carlo analysis to the rebinned UVES spectrum, i.e., at the same spectral resolution. To test whether or not the excited  $\text{Fe II } \lambda 2396 (J = 7/2)$  line observed in the LRIS spectrum could have been visible at the noise level of the UVES data, we considered “the relative position” defined as the sum of flux differences between two spectra over the pixel range along the  $\text{Fe II } \lambda 2396$  line profile. In Fig. 2, we plot the distribution of relative positions between the synthetic spectra and the LRIS spectrum. We compare it to the observed relative position,  $D_{\text{obs}}$ , between the UVES spectrum and LRIS spectrum. We find that  $< 0.1\%$  of the trials give  $D_{\text{obs}}$  as a result of random noise. This indicates that the UVES spectrum is statistically different from the LRIS spectrum and that the  $\text{Fe II } \lambda 2396$  line in the epoch 2 spectrum is significantly weaker than what is detected in epoch 1 spectrum. The observed difference is at greater than  $3\sigma$  level of significance.

The robustness of this result can be checked by considering a “control” spectral interval, chosen to be outside the  $\text{Fe II } \lambda 2396$  line profile and containing just the continuum. The Monte-Carlo analysis over this control interval shows that  $D_{\text{obs}}$  lies in the middle of the distribution of relative positions between the synthetic spectra and the LRIS spectrum – about 50% of values in the distribution are greater than  $D_{\text{obs}}$  and about 50% are lower. Hence, the UVES and LRIS spectra cannot be distinguished from each other in this control interval.

Table 1. Rest-frame Equivalent Widths of Fe II  $J = 7/2$  Transitions

	EW <sub>rest</sub> (Fe <sup>+</sup> , $J = 7/2$ ) [Å] <sup>a,b</sup>			
$\lambda$ [Å]	2333.516	2365.552	2389.358	2396.356
$f$	0.06917	0.04950	0.08250	0.26730
epoch 1 / LRIS	< 0.12	< 0.12	< 0.12	0.32 ± 0.06
epoch 2 / UVES	< 0.11	< 0.11	< 0.11	< 0.11

<sup>a</sup>Systematic errors in the continuum placement are included. They mainly affect the LRIS spectrum, while the UVES spectrum is dominated by the random noise.

<sup>b</sup>Upper limits are statistical,  $2\sigma$  non-detections.

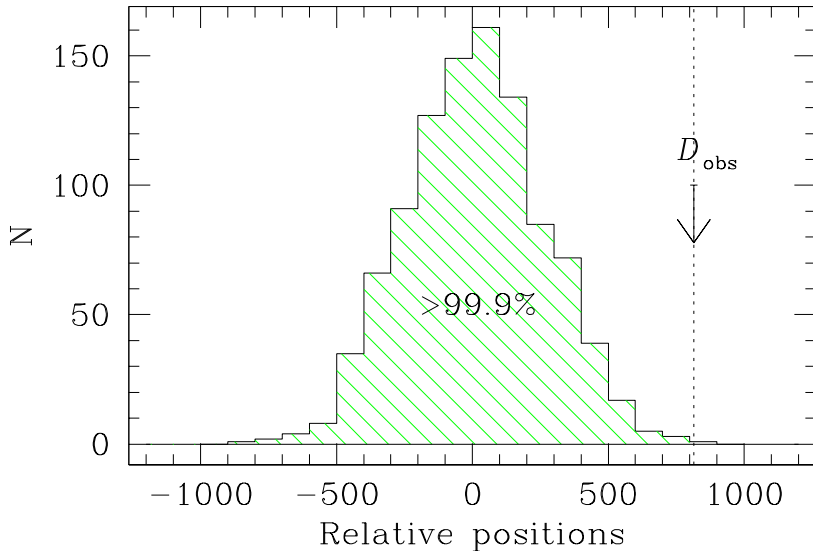


Fig. 2.— Distribution of the relative positions between 1000 synthetic spectra and the LRIS spectrum. The synthetic spectra were generated by random sampling of the LRIS data within the UVES noise (after the rebin of the UVES spectrum), and the relative position is defined as the sum of flux differences between two spectra over the pixel range along the Fe II  $\lambda 2396$  ( $J = 7/2$ ) line profile. The dotted line corresponds to the observed relative position,  $D_{\text{obs}}$ , between the rebinned UVES spectrum and the LRIS spectrum. We find that  $> 99.9\%$  of the chances  $D < D_{\text{obs}}$  in the distribution.

#### 4. Discussion

We have compared afterglow spectra of GRB 020813 obtained roughly 16 hours apart. Significant variation in the strength of the excited Fe II  $\lambda 2396$  feature identified in the GRB host is detected at  $> 3\sigma$  level of significance. A natural consequence of the excited lines being produced by UV pumping is that these excited levels are populated according to the flux of the radiation field. As the GRB afterglow fades, one must witness the decay of the excited states (PCB06). Our analysis of the afterglow spectra of GRB 020813 presents the first supporting evidence for the UV pumping model.

For the Fe<sup>+</sup> excited levels, the half-life for spontaneous emission is  $\approx 10$  minutes, significantly smaller than the characteristic decay time of the GRB afterglow (Fig. 3). Therefore, the population of the excited states of Fe<sup>+</sup> is expected to track the UV flux. At  $t_{\text{obs}} \approx 4.7$  and  $t_{\text{obs}} \approx 20.8$  hours, the excitation rates of the Fe II  $J = 7/2$  level due to indirect UV pumping are  $\approx 25 \text{ s}^{-1}$  and  $5 \text{ s}^{-1}$ , respectively. The excitation rates are estimated adopting the temporal declining index  $\alpha = -1.09$  from Li et al. (2003) and a spectral index  $\beta = -1$  from Covino et al. (2003). They are roughly consistent with the measured equivalent width and limit from the two-epoch observations.

Following PCB06, we find that the Fe<sup>+</sup> gas must lie beyond 40 pc from the GRB afterglow in

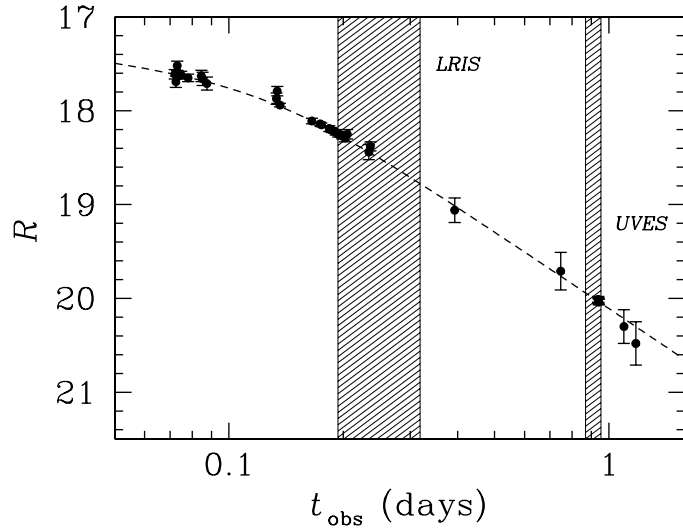


Fig. 3.— Observed  $R$ -band light curve for GRB 020813. Different photometric data are collected from Gladders & Hall (2002), Kiziloglu et al. (2002), Li et al. (2003), and Urata et al. (2003). The dashed curve is the smooth, double power-law model derived by Li et al. (2003) that best represents the decline of the afterglow light. Shaded area indicates the epochs when the spectroscopic data were taken.

order to survive the intense ionizing radiation field, but within 100 pc of the GRB afterglow such that it will significantly populate the  $\text{Fe}^+$  levels at  $t_{\text{obs}} \approx 4.7$  hours. In the case of GRB 020813, the absence of  $\text{Fe II } \lambda 2396$  at  $t_{\text{obs}} \approx 20.80$  hours further constrains the  $\text{Fe}^+$  gas at  $> 50$  pc from the afterglow. This is consistent with the presence of  $\text{Mg}^0$  identified in the host environment (Barth et al. 2003; Savaglio & Fall 2004) which implies a distance  $> 30$  pc (PCB06). The results presented here stress the value of obtaining both early and late-time observations of GRB afterglows. While acquiring the observations using the same telescope and instrument is preferred, we demonstrate that precise equivalent width measurements using data from different facilities can also yield strong constraints for the temporal evolution of the excited levels. Finally, a time-dependent calculation of radiative transfer and ion excitation may help further reveal the geometry and physical conditions of the gas.

The authors wish to acknowledge the ESO Science Archive Facility for the access to the UVES/VLT spectrum of GRB 020813. M.D.-Z. extends special thanks to S. Udry and F. Pont for useful discussions. H.-W.C. thanks ESO (Garching) for their hospitality during the writing of this manuscript. J.X.P. acknowledges helpful discussions with B. Mathews and R. Guhathakurta. J.X.P., H.-W.C., and J.S.B. are partially supported by NASA/Swift grant NNG05GF55G.

## REFERENCES

- Ballester, P., Modigliani, A., Boitquin, O., Cristiani, S., Hanuschik, R., Kaufer, A., & Wolf, S. 2000, *The Messenger*, 101, 31
- Barth, A. J., et al. 2003, *ApJ*, 584, L47
- Berger, E., Penprase, B. E., Fox, D. B., Kulkarni, S. R., Hill, G., Schaefer, B., & Reed, M. 2006, *ApJL*, submitted (astro-ph/0512280)
- Böttcher, M., Dermer, C. D., Crider, A. W., & Liang, E. P. 1999, *A&A*, 343, 111
- Chen, H.-W., Prochaska, J. X., Bloom, J. S., & Thompson, I. B. 2005, *ApJ*, 634, L25
- Covino, S., et al. 2003, *A&A*, 404, L5
- D’Odorico, S., Cristiani, S., Dekker, H., et al. 2000, in SPIE 4005, Discoveries and Research Prospects from 8- to 10-Meter-Class Telescopes, ed. J. Bergeron, 121
- Fiore, F., et al. 2005, *ApJ*, 624, 853
- Fox, D. W., Blake, C., & Price, P. 2002, *GCN Circ.* 1470

- Gladders, M., & Hall, P. 2002, GCN Circ. 1519
- Goodrich, R. W. 1995, *ApJ*, 440, 141
- Gull, T. R., Vieira, G., Bruhwiler, F., Nielsen, K. E., Verner, E., & Danks, A. 2005, *ApJ*, 620, 442
- Hall, P. B., et al. 2002, *ApJS*, 141, 267
- Kawai, N., et al. 2006, *Nature*, 440, 184
- Kiziloglu, U., et al. 2002, GCN Circ. 1488
- Lagrange-Henri, A. M., Vidal-Madjar, A., & Ferlet, R. 1988, *A&A*, 190, 275
- Li, W., et al. 2003, *PASP*, 115, 844
- Mirabal, N., et al. 2002, *ApJ*, 578, 818
- Oke, J. B., et al. 1995, *PASP*, 107, 375
- Perna, R., & Loeb, A. 1998, *ApJ*, 501, 467
- Prochaska, J. X., Chen, H.-W., & Bloom, J. S. 2006, *ApJ*, in press (PCB06; astro-ph/0601057)
- Prochaska, J. X., et al. 2006, *ApJS*, submitted
- Prochter, G. E., et al. 2006, *ApJL*, submitted (astro-ph/0605075)
- Ramirez-Ruiz, E., Graciá-Segura, G., Salmonson, J. D., & Pérez-Rendón, B. 2005, *ApJ*, 631, 435
- Savaglio, S., & Fall, S. M. 2004, *ApJ*, 614, 293
- Urata, Y., et al. 2003, *ApJ*, 595, L21
- van Marle, A. J., Langer, N., & Graciá-Segura, G. 2005, *A&A*, 444, 837
- Villasenor, J., et al. 2002, GCN Circ. 1471
- Vreeswijk, P. M., et al. 2001, *ApJ*, 546, 672
- Vreeswijk, P. M., et al. 2004, *A&A*, 419, 927
- Woosley, S. E., & Bloom, J. S. 2006, *ARA&A*, in press